J Mol Model (2013) 19:1739–1750
DOI 10.1007/s00894-012-1736-1

ORIGINAL PAPER

DFT study on the reactions of ClO^-/BrO^- with RCl (R = CH_3, C_2H_5, and C_3H_7) in gas phase

Liang Junxi · Wang Yanbin · Zhang Qiang · Li Yu · Geng Zhiyuan · Wang Xiuhong

Received: 7 September 2012 / Accepted: 13 December 2012 / Published online: 8 January 2013

Abstract Gas-phase reactions of ClO^-/BrO^- with RCl (R = CH_3, C_2H_5, and C_3H_7) have been investigated in detail using the popular DFT functional BHandHLYP/aug-cc-pVDZ level of theory. As a result, our findings strongly suggest that the type of reaction is firstly initiated by a typical S_N2 fashion. Subsequently, two competitive substitution steps, named as S_N2-induced substitution and S_N2-induced elimination, respectively, would proceed before the initial S_N2 product ion-dipole complex separates, in which the former exhibits less reactivity than the latter. Those are consistent with relevant experimental results. Moreover, we have also explored reactivity difference for the title reactions in term of some factors derived from methyl group, p-π electronic conjugation, ionization energy (IE), as well as molecular orbital (MO) analysis.

Keywords Anion ClO^-/BrO^- · Density functional theory (DFT) · Mechanism

L. Junxi · W. Yanbin (✉) · L. Yu
College of Chemical Engineering, Northwest University for Nationalities, Lanzhou, Gansu 730030, China
e-mail: wangyb16@yahoo.cn

L. Junxi
e-mail: liangjunxi@yahoo.cn

Z. Qiang (✉)
Institute of Arid Meteorology, CMA; Key laboratory of Arid Climatic Change and Reducing Disaster of Gansu Province, Key Open Laboratory of Arid Climatic Change and Disaster Reduction of CMA, Lanzhou 730020, China
e-mail: zhangqiang@cma.gov.cn

G. Zhiyuan · W. Xiuhong
Gansu Key Laboratory of Polymer Materials, College of Chemistry and Chemical Engineering, Key Laboratory of Eco-environment-related Polymer Materials; Ministry of Education, Northwest Normal University, Lanzhou, Gansu 730070, China

Introduction

Nucleophile ClO^-, a kind of familiar halogen-oxygen anion, was formed by CCl_4 and allowed to react with O originated from electron impact on N_2O [1]. Previously, a large amount of studies have been devoted to provide a wealth of insight concerning the anionic reactivity, [2–5] whether in the gas-phase or in solution. Besides, the reaction mechanisms induced by ClO^- have also received considerable attention, such as in the gas-phase reaction of ClO^- with RCl (R = methyl, ethyl, isopropyl and *tert*-butyl), the bimolecular nucleophilic substitution (S_N2) and base-induced bimolecular elimination (E2) pathways have been studied extensively by both experimentalists and theorists [6, 7]. Unfortunately, it is difficult to characterize the competition between S_N2 and E2 pathways because they lead to the same ionic products, which cannot be distinguished directly by experimental method [6, 8–19]. The reason has prompted Villano et al. [1] to reinvestigate the products derived from the reactions of ClO^- with RCl, on the basis of exploration of the analogous reactions, BrO^- + RCl, using the flowing afterglow-selected ion flow tube instrument (FA-SIFT) [20]. As a result, the same mechanism was proposed as the S_N2 and E2 processes, and an additional pathway, S_N2-induced substitution, was found for the BrO^- reactions. The cases were also recovered by Wladkowski and Brauman, [9] suggesting a secondary reaction occurs within the product ion/molecule complex from the reaction of CN^- with 2-chloropropionitrile. With those backgrounds, it seems interesting to undertake a detailed theoretical analysis to so estimate and predict the characters of the type of reactions initiated by S_N2 reactions [16], especially by S_N2 inducing reactions. Unfortunately, to the best of our knowledge, but for some MP2 level researches reported by Villano et al. [1] there are currently no theoretical studies on the additional reaction pathway that occurs after the S_N2 product ion-dipole complex. Thus, the principal thrust of the present work is to perform an investigation in theory to explore the mechanisms of the type

of anionic reactions; meanwhile, the results obtained can allow us to predict the analogous reaction properties for some known and/or as yet unknown systems.

It should be pointed out that comparative studies are very useful in understanding similarities and differences in chemical properties of molecules. In particular, trends in the properties of interest can often be more important than absolute values. In this paper, we aim at understanding how the halogen-oxygen anions react with some alkyl chloride on the basis of the simulation by the excellent DFT-BHandHLYP method. Accordingly, the reaction model of ClO^-/BrO^- + RCl (R = CH_3, C_2H_5, and C_3H_7) were chosen for our studying system, in which nucleophile reagents substituted by Cl/Br atoms possess similar properties, while the substrates represent a trend that can be studies as a function of the CH_3 group. As a purpose, through this theoretical work, we hope (i) to clarify the reaction mechanisms and to determine the structures and energetics of the intermediate complexes and transition states, as well as the characters of the substrates RCl, (ii) to investigate the thermodynamics of reactions of ClO^-/BrO^- with RCl molecules, (iii) to establish general trends and predictions for the reactions of ClO^-/BrO^- + RCl, and (iv) to compare reactivity between the ClO^- reaction and the BrO^- reaction.

Herein, in view of the previous experience that the energies and geometries computed with high-level ab initio methods such as QCISD, CCSD(T), and G3MP2 were similar to those obtained with the low-cost BHandHLYP method [21–23], we believe that the DFT-BHandHLYP calculations will provide an adequate theoretical level to this work, which is also fully confirmed by our calculations. As can be seen from Table 1, our work correlated well with the calculations performed by Villano et al. at a higher level of theory (MP2/aug-cc-pVDZ) [1], showing little difference between BHandHLYP and MP2 method, by 10 kJ mol^{-1}. To further assess the appropriateness of our means, reaction enthalpies $\Delta_r H_m^{\theta}$ at 298 K for the title reactions, ClO^-/BrO^- + RCl, have been additionally carried out at the DFT-BHandHLYP level using the large aug-cc-pVDZ basis. The results also demonstrate highly reliable conclusions comparing experimental evidences [24–26], with the largest deviation within 8 kJ mol^{-1} as shown in Table 1. Thus, our introduced approach should rationally adapt to this investigative system.

Computational methods

Geometries of all model complexes in this paper have been fully optimized at the BhandHLYP/aug-cc-pVDZ level [27–30]. For each optimized stationary point, vibrational frequency analysis based on the same level of theory was carried out to determine its character as either minima (the number of imaginary frequencies NIMAG = 0) or transition state structures (NIMAG = 1) and to evaluate the zero-point energy (ZPE) corrections, which are included in the relative energies. Moreover, the pathways between the transition structures and their corresponding minima have been characterized by intrinsic reaction coordinate (IRC) analyses [31]. The natural population analysis (NPA) has been made with the natural bond orbital (NBO) method [32] to obtain further insight into the bonding properties. All calculations reported here were performed using the Gaussian 03 suite of programs [33].

Results and discussion

Before the presentation of the calculated results for the title reactions, it is perhaps very worthwhile to define briefly the symbols for the anionic reactions. R-n, IM-X-n, TS-X-n and P-X-n are used to denote the reactants, intermediates, transition states and products, respectively. Here, the X is Cl or Br, indicating reactant is ClO^- or BrO^- anion, while n is the Arabic number, reflecting the higher number corresponds to the heavier R, such as number 3 represents the group C_3H_7 for R. With regard to the equilibrium geometries, Figs. 1, 2 and 3 have described clearly, with structural data given to some primary atoms. Moreover, to simplify the comparisons and to emphasize the trends, we have given the potential energy profiles that, starting reactants R that is set at zero as a reference, are vividly depicted in Fig. 4, which are taken from the BhandHLYP level as summarized in Table 1. Figure 5 provides the energy profiles of all paths that resulted from IRC calculations, in which the minimum energy pathways connect the TSs to loosely bound dipole-dipole complexes in both the forward and backward directions.

Reaction pathway of ClO^-/BrO^-

As can be seen from Figs. 1, 2 and 3 together with Fig. 4, the type of reactions is firstly initiated by a typical S_N2 reaction where the backside nucleophilic attack of anion at the carbon atom (S_N2(C)) with concerted expulsion of the leaving group Cl^-. Later, the two competitive substitutions would proceed before the initial S_N2 product ion-dipole complex separates, which was traced to the fact that the thermodynamics of the system make the lifetime of these complexes relatively long, allowing for additional chemistry to occur [34]. To make our discussion more convenient, one is named as S_N2-induced substitution according to the behavior of corresponding TS that resembles traditional bimolecular nucleophilic substitution, while another is rationally expressed as S_N2-induced elimination on the basis of transition vector of its TS. Thus,

Table 1 Energies of the various geometries for the reaction pathways (total energy E_T (electronic + zero point energy), relative energy E_R (in normal font), and reaction enthalpies $\Delta_r H_m^{\theta}$ at 298 K (in italic font))

Species	CH_3Cl		C_2H_5Cl		C_3H_7Cl	
	E_T(a.u.)	E_R(kJ mol^{-1})	E_T(a.u.)	E_R(kJ mol^{-1})	E_T(a.u.)	E_R(kJ mol^{-1})
ClO^- reactions						
R	−1035.517745	0.00	−1074.810506	0.00	−1114.103664	0.00
IM1	−1035.536330	−48.80 (−50.21) [a]	−1074.830249	−51.84	−1114.125723	−57.92
IM2	−1035.574167	−148.14 (−158.99) [a]	−1074.869758	−155.57	−1114.164825	−160.58
IM2'	−1035.664751	−385.97 (−397.48) [a]	−1074.959035	−389.96	−1114.257994	−405.19
IM2"	−1035.573876	−137.37 (−150.62) [a]	−1074.868627	−142.60	−1114.156376	−148.40
TS1	−1035.533294	−40.82 (−37.66) [a]	−1074.822982	−32.76	−1114.113929	−26.95
TS1'	−1035.573876	−147.37 (−133.89) [a]	−1074.868630	−152.61	−1114.163371	−156.76
TS1"	−1035.556336	−101.32 (−92.05) [a]	−1074.850654	−105.41	−1114.140001	−95.40
P1	−1035.555940	−100.28 (−108.78) [a]	−1074.849996	−103.68	−1114.144714	−107.78
		−86.86 (−83.68) [d]		*−93.88 (−92.05)* [d]		*−97.52 (−92.05)* [d]
P2	−1035.613365	−251.05 (−263.59) [a]	−1074.917488	−280.88	−1114.217996	−300.18
		−237.65 (−234.30) [d]		*−280.47 (−276.15)* [d]		*−294.20 (−288.70)* [d]
P3	−1035.555940	−100.28 (−108.78) [a]	−1074.849996	−103.68	−1114.144714	−107.78
		−86.86 (−83.68) [d]		*−93.88 (−92.05)* [d]		*−97.52 (−92.05)* [d]
BrO^-reactions						
R	−3149.470065	0.00	−3188.762826	0.00	−3228.055984	0.00
IM1	−3149.487717	−46.35	−3188.781506	−49.04	−3228.077733	−57.10
IM2	−3149.525063	−144.40	−3188.821024	−152.80	−3228.116274	−158.29
IM2'	−3149.595116	−328.32	−3188.900462	−361.36	−3228.204010	−388.64
IM2"	−3149.508842	−101.81	−3188.815857	−139.23	−3228.110688	−143.63
TS1	−3149.483675	−35.73	−3188.774252	−30.00	−3228.063970	−20.97
TS1'	−3149.524547	−143.04	−3188.819404	−148.55	−3228.114615	−153.94
TS1"	[b]	[b]	−3188.800499	−98.91	−3228.089510	−88.02
P1	−3149.506498	−95.66	−3188.800531	−99.00	−3228.093969	−99.73
		−91.05 (−87.86) [c]		*−98.93 (−96.23)* [c]		*−99.39 (−96.23)* [c]
P2	−3149.563258	−244.68	−3188.867381	−274.51	−3228.167889	−293.81
		−239.36 (−246.86) [d]		*−281.18 (−288.70)* [d]		*−281.91 (−276.15)* [d]
P3	−3149.505833	−93.91	−3188.799889	−97.31	−3228.094607	−101.41
		−94.58 (−96.23) [d]		*−99.56 (−104.70)* [d]		*−101.23 (−104.70)* [d]

[a] Relative energies calculated at the MP2/aug-cc-pVDZ level of theory are from ref 1

[b] Nonexistent due to uncertain TS

[c] Ref 24

[d] Ref 25

the discussions of all transition states as well as the reactive intermediates might be very interesting and quite important for the title reactions.

As a comparison, we predicted the very similar mechanism and trend for both the ClO^- reactions and the BrO^- reactions, in which each step is very favorable thermodynamically, especially S_N2-induced elimination as shown in Fig. 4. Also, for a given neutral reagent, the reactions of ClO^- are more efficient than those of BrO^-, which supports the fact that the BrO^- anion has weaker basicity than the ClO^- anion [1]. More detailed information will be elucidated in the following sections.

Intermediate IM-X-n

The first intermediates (IM1-X-n) are a type of weakly bonded complexes due to the electrostatic effect of the XO^- close up to the RCl, in excellent agreement with the nature of anion reactions [35–39]. When compared with the

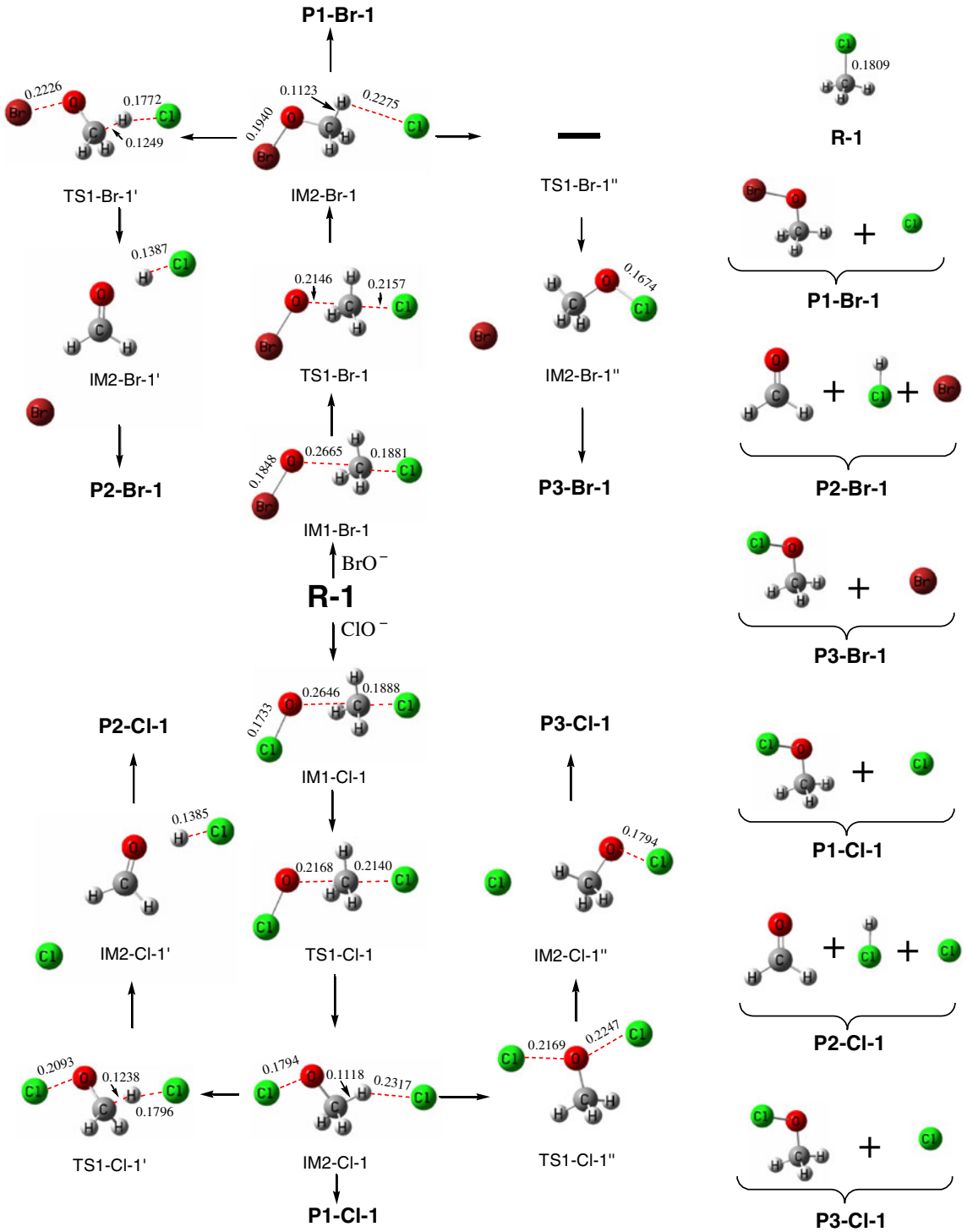

Fig. 1 Optimized geometries of the reactions of CH_3Cl with ClO^-/BrO^- at the BHandLYP/aug-cc-pVDZ level of theory (the symbol "—" denotes the uncertain TS on PES), with bond distances in nm

isolated reactants, as shown in Figs. 1, 2 and 3, the "precursor" complexes are almost unperturbed in geometries and so take on more reactant–like characters. Also, it is noted that the bound C-Cl distances in RCl moiety is already activated, reflecting slight stretch with respect to reactant RCl. As has been well established by NBO charges analysis as indicated in Table 2, the quantum charges transfer in the complexes, $[XO^-\cdots RCl]$, already exist, which help the reactions to proceed subsequently. BHandHLYP complexation energies ΔE_{comp} obtained

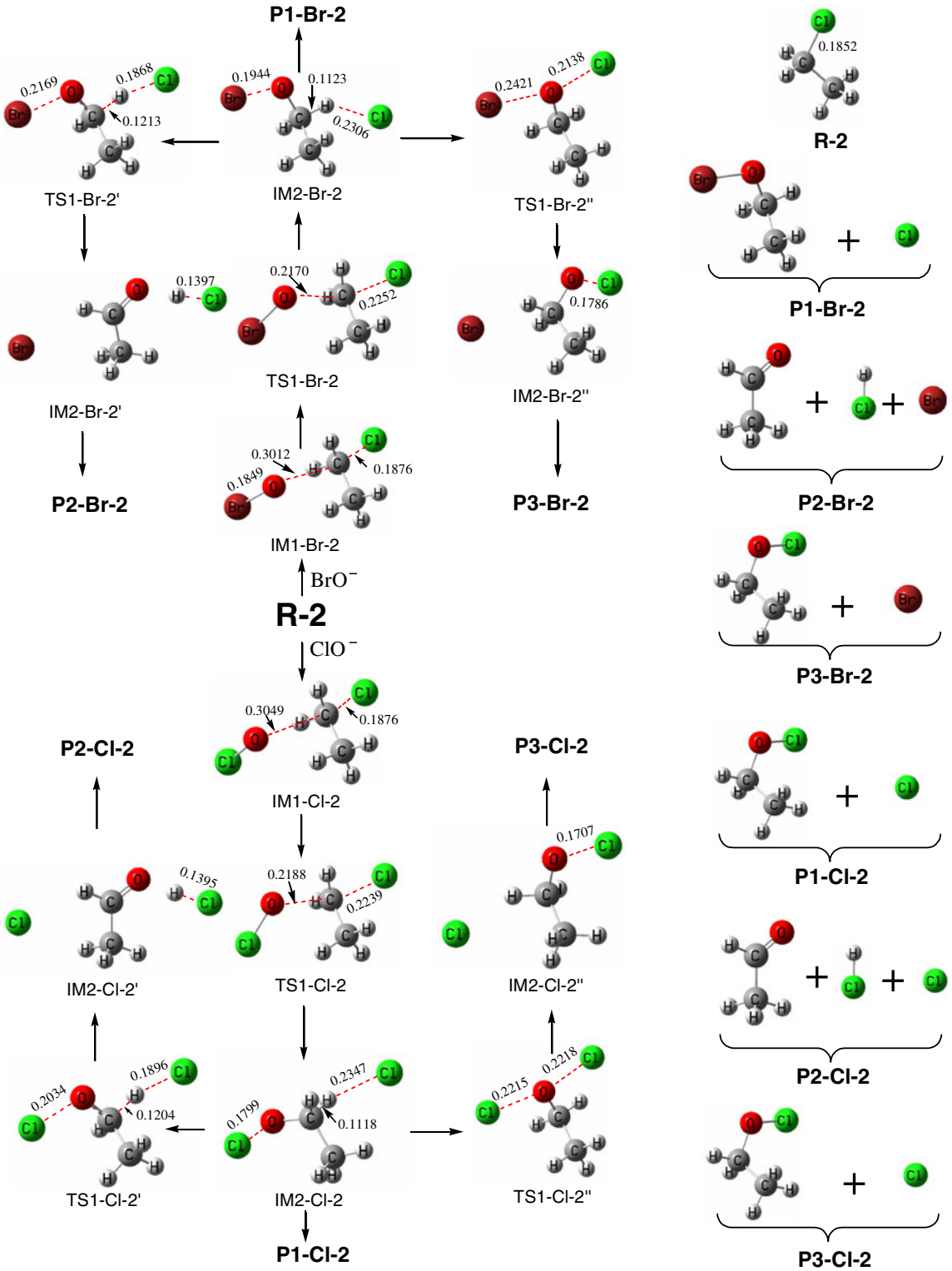

Fig. 2 Optimized geometries of the reactions of C_2H_5Cl with ClO^-/BrO^- at the BHandLYP/aug-cc-pVDZ level of theory, with bond distances in nm

for the IM1s, as shown in Table 1, are identically negative and corresponding strength is predicted to be in the order (kJ mol^{-1}) IM1-Cl-3 (−57.92) > IM1-Cl-2 (−51.84) > IM1-Cl-1 (−48.80) and IM1-Br-3 (−57.10) > IM1-Br-2 (−49.04) > IM1-Br-1 (−46.35). Those strongly suggest that the formation of all complexes is without barriers and corresponding stabilization difference is associated with the size of both reactants.

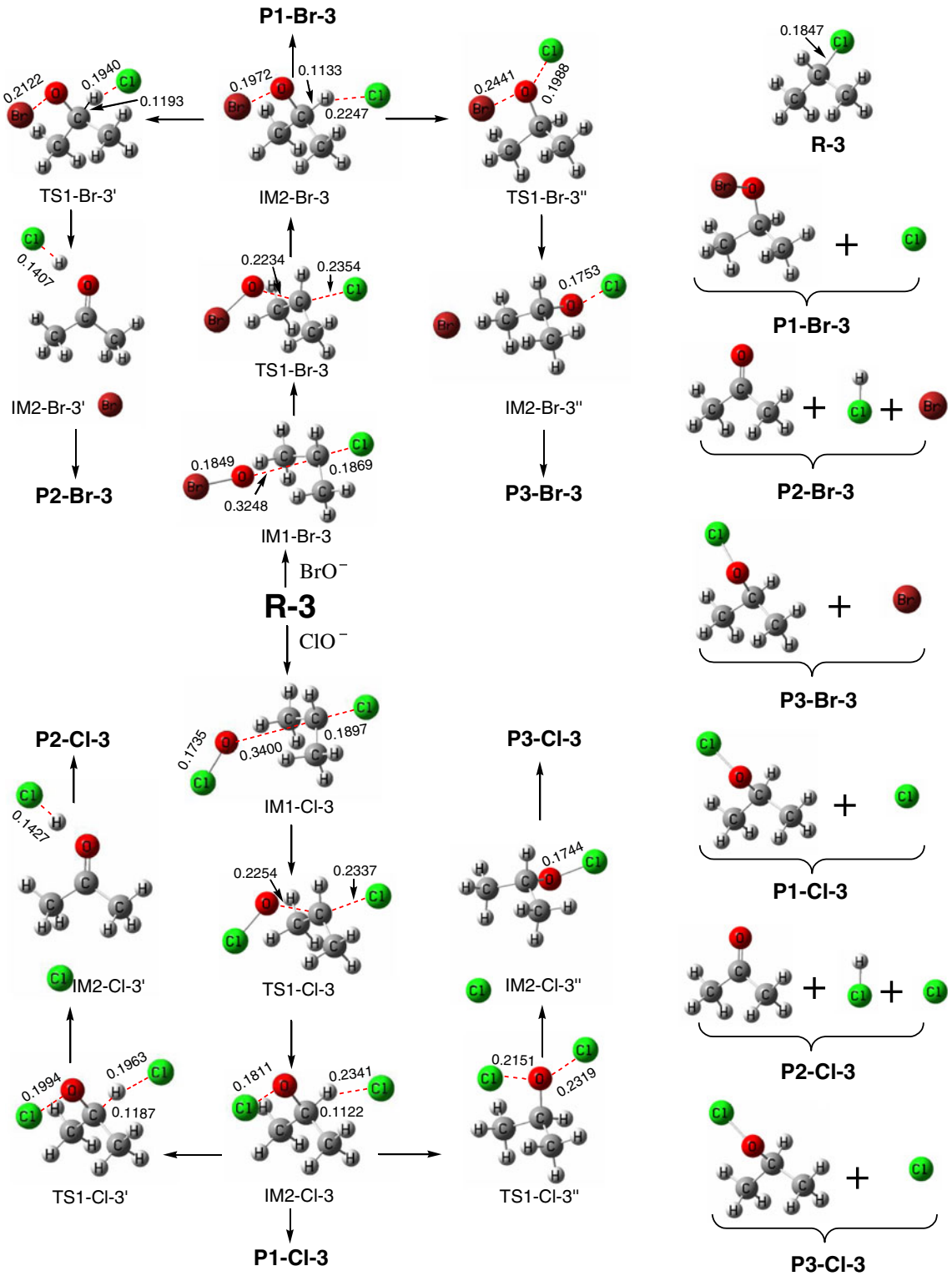

Fig. 3 Optimized geometries of the reactions of C_3H_7Cl with ClO^-/BrO^- at the BHandLYP/aug-cc-pVDZ level of theory, with bond distances in nm

However, we unexpectedly reveal that the trend in dipole moment (D) also mirrors the trend in ΔE_{comp}: IM1-Cl-3 (6.3482) > IM1-Cl-2 (5.7900) > IM1-Cl-1 (4.4712) and IM1-Br-3 (3.1636) > IM1-Br-2 (2.8182) > IM1-Br-1 (2.1587) as presented in Table 2. This result seems to disagree with Wiberg et al.'s investigation [40] in which the conformation with the smaller dipole moment may increase its relative stability. Presumably this is because of the

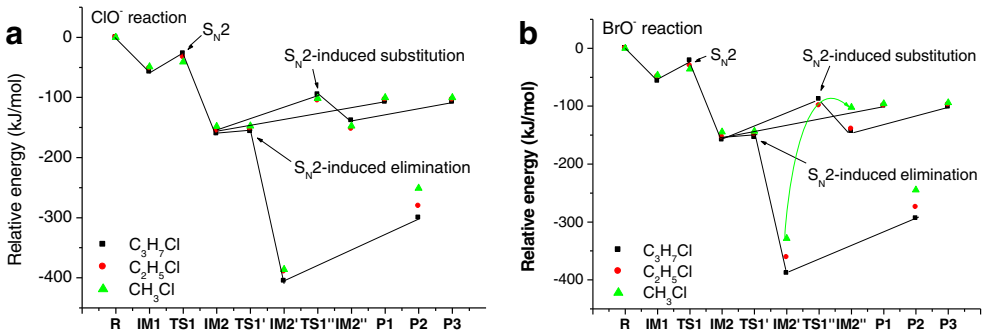

Fig. 4 Energy profiles for the ClO^- reactions (**a**) and BrO^- reactions (**b**), respectively. The relative energies are taken from the BHandLYP/aug-cc-pVDZ level of theory as given in Table 1. Note that the transition state for the S_N2-induced substitution reaction of CH_3Cl + BrO^- failed to be located on PES

fact that the complexes molecules, IM1-X-n, are all weakly bonded species. To understand the trend of dipole moment for IM1-X-n, it is fairly reasonable if we consider the decrease in electronegativity from Cl to Br atoms. The IM1-Cl-1 molecule is expected to have the largest charge separation. However, the dipole moment also depends on the bond distance, and in this case, the IM1-Cl-3 molecule possesses longer bonds than the IM1-Cl-1 and IM1-Cl-2 molecules.

The second intermediates (IM2-X-n), a type of ion-dipole complexes, are formed easily via a S_N2 step from the energetic viewpoint. The complexes consist of two moieties XOR + Cl^-, where the displaced Cl^- anion is positioned behind the XOR group, facilitating either abstraction of hydrogen atom or attack on oxygen atom. Thus, the intermediates are not only the products ion-dipole of initial S_N2 well, but also the reactant complexes for succeeding reactions. As mentioned in the preceding section "Reaction pathway of ClO^-/BrO^-", since lifetimes of the complexes are relatively long [34], the IM2-X-n should possess stronger stabilization, which is borne out by our BHandHLY calculations. As shown in Table 1, complexes IM2s lie not less than 144.40 kJ mol^{-1} below the energy of the separate reactants, whether the ClO^- reactions or the BrO^- reactions, with a value which is around 100 kJ mol^{-1} smaller in energy than the corresponding IM1s. The other striking feature is the dipole moment, indicating the IM2s are bigger than IM1s as shown in Table 2, so proposing more dipole for IM2s in structure. Those determine the possibility of the IM2s to process succeeding reactions. Namely, our theoretical findings suggest that the Cl^- products of reactions of ClO^- were produced not only from the S_N2 reactions, but also from other reaction paths, such as S_N2-induced substitution and S_N2-induced elimination reported by Villano and co-workers [1].

The third intermediates are all ion-dipole complexes but have two kinds of different structure. As shown in Figs. 1, 2 and 3, one expressed by the symbol IM2-X-n' consists of three monomers which are gained by S_N2-induced elimination, while the other (via S_N2-induced substitution) by IM2-X-n" involves two moieties. As a comparison, relative energies of the former are much smaller than those of the latter, especially the former, IM2-X-n', that has the lowest on PES among all stationary points presented here, as can be seen from Fig. 4. Moreover, whether the former or the latter, the stability is significantly influenced not only by the bulk of the substrates, but also by the substitutes of the anions. Taking the former as an illustrative example, as shown in Table 1, IM2'-Cl-3 (−388.64) > IM2'-Cl-2 (−361.36) > IM2'-Cl-1 (−328.32) and IM2'-Br-3 (−405.19) > IM2'-Br-2 (−389.96) > IM2'-Br-1 (−385.97).

Transition state TS-X-n

Now, we turn our attention to the corresponding transition states TSs. For TS1-X-n described as the typical S_N2 fashion, the examination of the single imaginary frequency for each TS provides excellent confirmation of the concept of the S_N2 process. In Fig. 5, we give the potential energy profiles for corresponding TSs along the reaction coordinates. Note that all transition states were relatively "early" TSs for corresponding reactions, in which the degree is progressively weak as n varies from 1 to 3, suggesting that the S_N2 takes place earlier for the lighter substrate analogues. In other words, TS1-X-1 is more reactant-like and TS1-X-3 is more product-like. This prediction was fully estimated by the structural trend. As can be seen from Figs. 1, 2 and 3, for TS1-Cl-n an increasingly stretched carbon–leaving bond (C-Cl; nm) changes from 0.2140 to 0.2239 to 0.2337 while from 0.2157 to 0.2252 to 0.2354 for TS1-Br-n, as n varies from 1 to 3. At the same point, the formation bonds (O-C; %) were shortened about 18 (TS1-Cl-1), 28 (TS1-Cl-2), 34 (TS1-Cl-3) and 19 (TS1-Br-1), 30 (TS1-Br-2), 37 (TS1-Br-3), from corresponding starting complexes IM1-X-n. Consequently, a smaller barrier should be the reaction with TS1-X-1 [41], in which the ClO^- reactions are more reactive than the BrO^- reactions. Taking TS1-Cl-n as an illustrative example, TS1-Br-n is analogous. As shown in Table 1, the energy barrier for ClO^- + CH_3Cl reaction is only 7.98 kJ mol^{-1}, with 19.08 kJ mol^{-1} for ClO^- + C_2H_5Cl reaction and 30.97 kJ mol^{-1} for ClO^- + C_3H_7Cl reaction. Thus, our calculation compares well with the previous conclusions that nucleophiles limited to S_N2

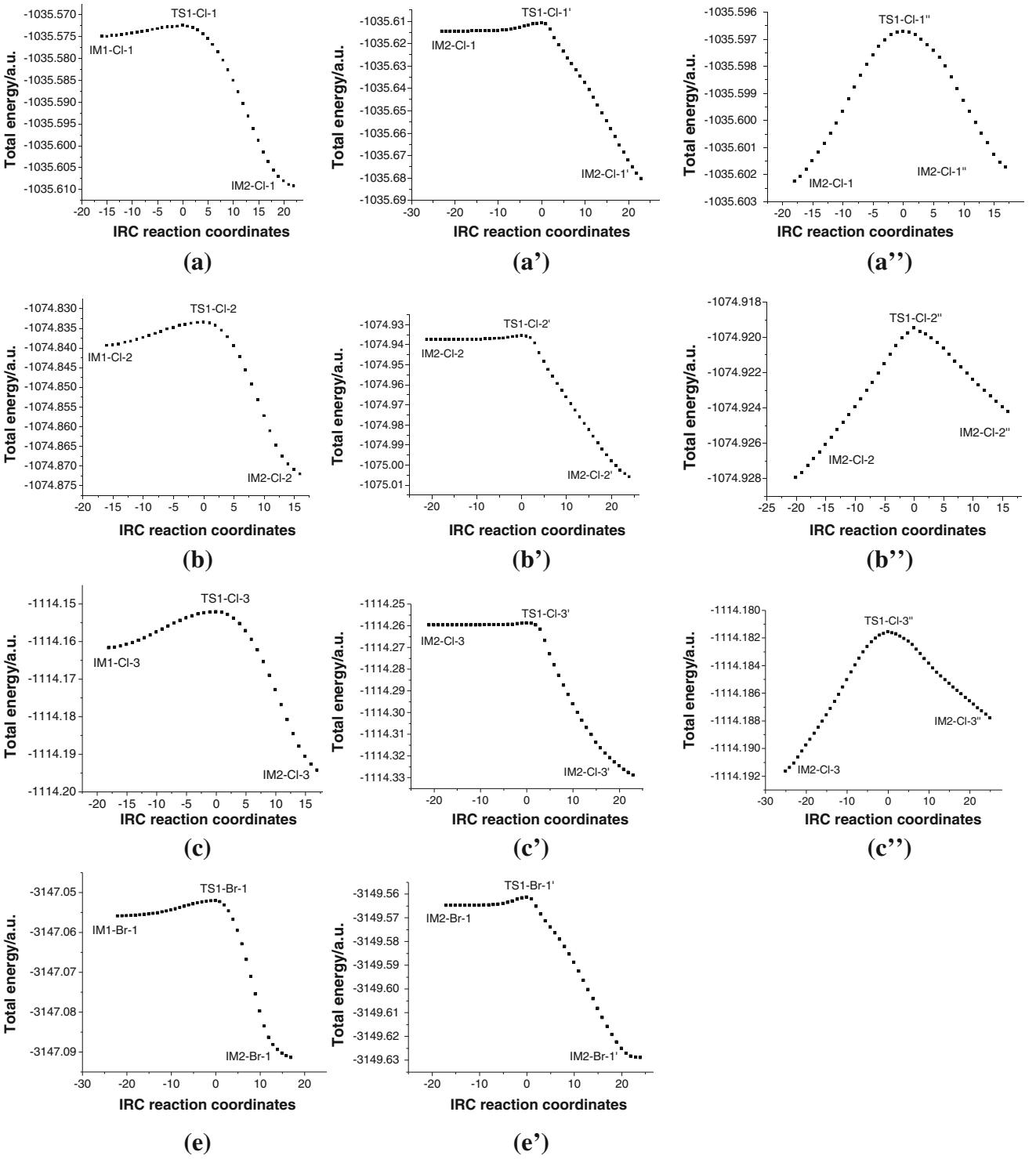

Fig. 5 Potential energy profiles for the associated pathways along the coordinates

processes may give the rate decrease with more highly substituted alkyl halides [12, 13].

The second TS gives some insight into two different transition state fashions, TS1-X-n' and TS1-X-n". As is displayed in Figs. 1, 2 and 3, the former by S_N2-induced elimination is that Cl abstracts an H atom from the alkyl of ROX, displacing X and forming a C–O double bond, which is similar to a previous report for alkyl nitrites reactions [18]. While the latter by S_N2-induced substitution is that Cl attacks the oxygen atom of ROX (X = Cl and Br) displacing X. In general, localized bases favored elimination and delocalized nucleophiles favored substitution [16]. As a result, X^- goes mainly along

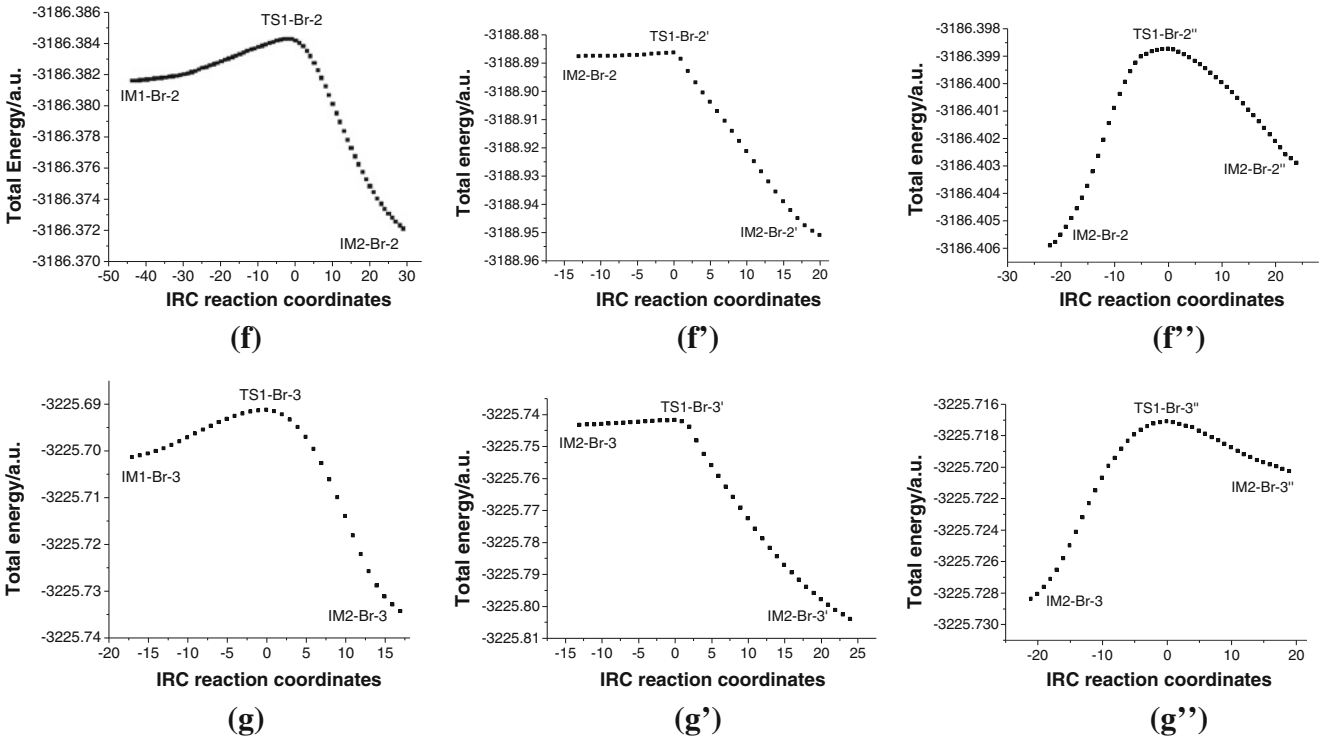

Fig. 5 (continued)

the elimination reactions, which is fully confirmed by our BhandHLYP calculation. As shown in Table 1, the relative energies indicated that TS1-X-n' are significantly smaller than TS1-X-n", and slightly larger in comparison with IM2-X-n. Those support well Villano et al.'s investigative results [1], proposing the occurrence of S_N2-induced elimination is favored dynamically.

In this paper, we give the potential energy profiles for corresponding TSs along the reaction coordinates. As can be seen from Fig. 5, the energy profiles for the TS1-X-n' system coincide with each other, reflecting the relatively "early" TSs. In contrast, the relatively "late" features are demonstrated in the TS1-X-n" system, in which the reactions reach the TS gradually late in the sequence n = 1, 2, 3,

Table 2 The charges and dipole assigned to complexes IM-X

			XO^-	C_3H_7Cl	XO^-	C_2H_5Cl	XO^-	CH_3Cl
NBO charges (a.u.)	IM1-Cl		-0.952	-0.048	-0.944	-0.056	-0.928	-0.072
	IM1-Br		-0.956	-0.044	-0.962	-0.048	-0.938	-0.062
Dipole (D)	IM1	ClO^-	6.3482		5.7900		4.4712	
		BrO^-	3.1636		2.8182		2.1587	
	IM2	ClO^-	9.8508		10.1565		10.2140	
		BrO^-	11.5763		12.6528		13.1339	
Fragment orbital overlap (kJ mol^{-1})								
⟨HOMO|LUMO⟩		ClO^-	47.26		36.76		34.13	
		BrO^-	65.64		55.14		52.51	
[a] Ionization energy (IE)		ClO^-	225.98	[b] NBO charges populations	Cl		0.370	*-0.094*
					O		-0.370	*-0.906*
		BrO^-	233.13		Br		0.451	*-0.043*
					O		-0.451	*-0.957*

[a] Values are reported in kJ mol^{-1} at the BHandHLYP level

[b] Computed NBO charges (a.u.) populations on each atom of OX molecules on their radical anionic (in italic font) and neutral states (in normal font) at the BHandHLYP/aug-cc-pVDZ level

with the increasing endothermicity in terms of Hammond postulate [41]. Thus, if the reaction exceeds a certain exothermicity or endothermicity, the TS merges with the Rea or Pro, respectively [42]. As expected, a single-well PES on the reaction profile was revealed for TS1-Br-1" system in which repeated attempts to find TS using the DFT methodology failed. Our theoretical investigations therefore suggest that no TS exist on the BhandHLYP/aug-cc-pVDZ surface for the S_N2-induced substitution reaction of BrO^- with CH_3Cl, which agrees well with the investigative results by Villano [1], proposing the occurrence of the S_N2-induced elimination mechanism rather than the double substitution mechanism.

Reactivity analysis

Our aim is to understand *why*, for a given substrate, each stationary point involving ClO^- relative to BrO^- is low on PES and *why*, for a given anion reagent, energy barrier increases as the substrate is varied from CH_3Cl to C_3H_7Cl.

The effect analysis from substrate

Methyl group effect, exhibiting the electron-donation ability, is very remarkable for the geometry difference. For instance, as shown in Figs. 1, 2 and 3, the bound C-Cl distance in the substrates ranges from 0.1809 nm (CH_3Cl) to 0.1852 nm (C_2H_5Cl), stretching about 2 %. This is mainly because of the existence of methyl group that contributes to the C-Cl bond of C_2H_5Cl longer derived from electrons flowing into C-Cl σ^* antibonding orbital. Note that C_3H_7Cl (0.1847) has a shorter C-Cl bond distance than C_2H_5Cl (0.1852), implying that the ability of the p-π electronic conjugation effect appearing in C_3H_7 group is greatly dominant. Thus, we have inferred that molecular reactivity is ruled by the dual effect, both electron-donation and p-π electronic conjugation. Nevertheless, these results do not essentially influence our calculated results, proposing the barriers are increasing as the substrate from CH_3Cl to C_3H_7Cl, as shown in Fig. 4. According to NBO analysis that, taking the TS1-Cl-n as an example as listed in Table 3, the largest stabilization energies (the sum of 76.36 kJ mol^{-1}) indicate that the dominant hyperconjugative interaction exists in TS1-Cl-3 system, which tends to hinder the elimination of the Cl atom. Likewise, one can see that methyl group effect is responsible for the stabilization of the TS1-X-n system, reflecting the molecule with more CH_3 group has the more steady structure. Moreover, it is also noted that all the S_N2-induced elimination reactions present a lower barrier than the S_N2-induced substitution reactions and the reactivity is decreased with the substrate from CH_3Cl to C_3H_7Cl, which has been successfully borne by the NBO analysis. As shown in Table 3, in TS1-X-n' the donation of LP (Cl^{**}) into the antibonding orbital of C-H (LP (Cl^{**})→σ^*(C-H)) seems to give the stronger stabilization, compared with in TS1-X-n" (LP (X^*)→σ^*(O-Cl)). Here, Cl^{**} denotes the chlorine that abstraction forward H atom, X^* denotes the leaving atom X. More important, in TS1-X-n' the interaction for LP (Cl^{**})→σ^*(C-H), playing a critical role in process of H-atom shift, becomes distinctly weak in the sequence RCl = CH_3Cl, C_3H_7Cl, C_3H_7Cl.

Table 3 NBO analysis for all TSs obtained at the BHandHLYP/aug-cc-pVDZ level

σ_{donor}	$\sigma^*_{acceptor}$	[a] $E(2)$ (kJ mol^{-1})					
S_N2 reaction		TS1-Cl-1	TS1-Br-1	TS1-Cl-2	TS1-Br-2	TS1-Cl-3	TS1-Br-3
LP (O)	σ^*(C-Cl)	28.53	24.98	5.19	6.82	0.33	0.29
$^1\sigma$(C-H)	σ^*(C-Cl)	5.90	5.86	33.43	32.89	35.03	34.06
$^2\sigma$(C-H)	σ^*(C-Cl)	5.69	5.65	5.77	5.77	34.98	33.01
$^3\sigma$(C-H)	σ^*(C-Cl)	5.69	5.65	5.61	5.73	6.02	5.94
S_N2-induced elimination		TS1-Cl-1'	TS1-Br-1'	TS1-Cl-2'	TS1-Br-2'	TS1-Cl-3'	TS1-Br-3'
LP (Cl^{**})	σ^*(C-H)	45.94	50.17	36.57	41.09	30.79	34.39
$\sigma(C^2$-H)	σ^*(C-H)	—	—	9.87	9.96	21.25	21.17
$\sigma(C^1$-$C^2)$	σ^*(C-H)	—	—	3.56	3.39	9.37	9.12
σ(X-O)	σ^*(C-H)	17.70	19.58	14.90	16.90	13.93	15.77
S_N2-induced substitution		TS1-Cl-1"	TS1-Br-1"	TS1-Cl-2"	TS1-Br-2"	TS1-Cl-3"	TS1-Br-3"
LP (X^*)	σ^*(O-Cl)	5.10	—	7.32	5.31	1.63	0.92
$\sigma(C^1$-H)	σ^*(O-Cl)	25.77	—	29.83	29.08	12.38	10.21
$\sigma(C^1$-$C^2)$	σ^*(O-Cl)	—	—	—	—	11.46	12.13
$\sigma(C^1$-O)	σ^*(O-Cl)	9.41	—	11.76	6.82	6.65	3.72

[a] $E(2)$ is the perurbative analysis hyperconjuagtive energy, $^1\sigma$(C-H), $^2\sigma$(C-H) and $^3\sigma$(C-H) possess the same C atom for TS1-Cl-1; $^2\sigma$(C-H) and $^3\sigma$(C-H) but $^1\sigma$(C-H) possess the same C atom for TS1-Cl-2; $^1\sigma$(C-H), $^2\sigma$(C-H) and $^3\sigma$(C-H) possess a different C atom for TS1-Cl-3 . The symbol C^1 denotes the carbon that bonded to O atom; C^2 denotes the carbon that bonded to C^1 ; Cl^{**} denotes the chlorine that abstraction forward H atom; X^* denotes the leaving atom X. The symbol "—" denotes the nonexistent values

IE analysis from anion

As mentioned above, our DFT calculations predict that the reactions of BrO^- are less efficient than those of ClO^-. This is due to the weaker basicity of the BrO^- anion (1479.05 kJ mol^{-1}) relative to the ClO^- anion (1487.83 kJ mol^{-1}) [43], which is further confirmed by our IE-calculation. As listed in Table 2, BrO^- compared with ClO^- has a slightly high value in IE, 233.13 kJ mol^{-1} vs. 225.98 kJ mol^{-1}, implying a stronger reactivity for ClO^- when the substrate is fixed. Moreover, for the two anions the halogens would interact with the oxygen atom through the oppositely operating electronic effects, mesomeric (+M)-π donor and inductive (-I)-σ acceptor. In terms of Pauling electronegativities [44], the Br (2.96) becomes less electronegative than the Cl (3.16), and thus has less capability to withdraw charge from the central oxygen atom. As a result, for ClO^-, the (-I)-σ acceptor is preferred over (+M)-π donor, while the reverse is true for BrO^-. However, with respect to Br atom, since Cl atom possesses smaller size, the electrons prefer flowing to the oxygen p-orbital, increasing the nucleophilicity of the anion. This case can be well rationalized by our NBO analysis that indicates, as listed in Table 2, there is 0.030 a.u. more electronic distribution on oxygen atom of ClO^- than on that of BrO^- in the process of XO^- forming derived from neutral counterparts. Those show a fairly close correspondence in our prediction, proposing that the ClO^- reactions are highly reactive, in comparison with the BrO^- reactions.

Molecular orbital (MO) analysis of the BrO^-/ClO^- + RCl (X = CH_3, C_2H_5 and C_3H_7) model system

Our discussion will focus on the relevant molecular orbitals for the BrO^-/ClO^--induced reactions, which are determined by the donor–acceptor orbital interactions between occupied O (BrO^-/ClO^-) $2p_z$ AOs and the empty σ^* C–Cl acceptor orbital in the substrates RCl (R = CH_3, C_2H_5 and C_3H_7). Fragment orbital overlap ⟨Anion|Substrate⟩ analysis has been successful in understanding this kind of reaction. As shown in Table 2, the differential orbital energies, ⟨HOMO|LUMO⟩, between the reagent BrO^-/ClO^- HOMO orbital and the substrate RCl (R = CH_3, C_2H_5 and C_3H_7) LUMO orbital fall in the order $\langle ClO^- \mid C_3H_7Cl\rangle > \langle ClO^- \mid C_2H_5Cl\rangle > \langle ClO^- \mid CH_3Cl\rangle$ for the ClO^- system and $\langle BrO^- \mid C_3H_7Cl\rangle > \langle BrO^- \mid C_2H_5Cl\rangle > \langle BrO^- \mid CH_3Cl\rangle$ for the BrO^- system, and the values of $\langle ClO^- \mid RCl\rangle$ are usually smaller than those of the corresponding $\langle BrO^- \mid RCl\rangle$. According to the accepted theory [45–48], a small differential orbital energy can lead to an easier reaction due to the lower TS interaction $\Delta E^{\neq}_{int}$. A better ⟨HOMO|LUMO⟩ interaction for BrO^-/ClO^- + RCl is associated with the size of the substituent R in the substrate, that is, the reactivity for both BrO^- + RCl and ClO^- + RCl is increasingly strengthened as R is changed from C_3H_7 to CH_3, and the reactions of ClO^- are usually preferred over the reactions of BrO^-.

Conclusions

In summary, the reaction mechanisms of ClO^-/BrO^- with RCl (R = CH_3, C_2H_5, and C_3H_7) have been analyzed in detail and the influence of the substitution on the intermediates, transition states, energetics, geometrical parameters, etc., have been comparatively investigated at the DFT-BHandHLYP level of theory using aug-cc-pVDZ basis set. The following conclusions have been drawn: (1) The reaction is firstly initiated by a typical S_N2 fashion. Later, the two competitive substitutions, named as S_N2-induced substitution and S_N2-induced elimination, would proceed before the initial S_N2 product ion-dipole complex separates, where the former exhibit less reactivity than the latter. (2) A single-well PES only appears for the S_N2-induced substitution of reaction of BrO^- + CH_3Cl, in comparison with the analogous reactions presented here. (3) Reactivity of the substrate molecules is ruled by the dual effect from both methyl group effect and p-π electronic conjugation appearing in C_3H_7 group. (4) According to MO analysis, whether the BrO^- reactions or the ClO^- reactions, the reactivity progressively increases as the R-substitution of substrates RCl is changed from C_3H_7 to CH_3, with the reactions of ClO^- usually preferred over the reactions of BrO^-, which is also rationally confirmed from IE analysis.

Project supported: The Scientific and Technical Project Supported by Gansu Province (Project No. 090GKCA027), The Scientific and Technical Project of Lanzhou City (Project No. 2009-1-167), Science Fund of Public Welfare Meteorological Organization (Project No. GYHY200806021 and GYHY201106029), National Basic Research Program of China (Project No. 2012CB955304), the National Key Natural Science Fund (Project No. 40830957), and National Natural Science Fund (Project No. 41261052).

References

1. Villano SM, Eyet N, Lineberger WC, Bierbaum VM (2009) J Am Chem Soc 131:8227–8233
2. Mackay GI, Bohme DK (1978) J Am Chem Soc 100:327–329
3. Olmstead WN, Brauman JI (1977) J Am Chem Soc 99:4219–4228
4. Brauman JI, Blair LK (1970) J Am Chem Soc 92:5986–5992
5. Brodbelt JS, Isbell J, Goodman JM, Secor HV, Seeman JI (2001) Tetrahedron Lett 42:6949–6952
6. Villano SM, Kato S, Lineberger WC, Bierbaum VM (2006) J Am Chem Soc 128:736–737
7. Hu WP, Truhlar DG (1996) J Am Chem Soc 118:860–869
8. Lieder CA, Brauman JI (1975) Int J Mass Spectrom Ion Process 16:307–319
9. Wladkowski BD, Brauman JI (1992) J Am Chem Soc 114:10643–10644

10. Lum RC, Grabowski JJ (1988) J Am Chem Soc 110:8568–8570
11. Jones ME, Ellison GB (1989) J Am Chem Soc 111:1645–1654
12. Gronert S, DePuy CH, Bierbaum VM (1991) J Am Chem Soc 113:4009–4010
13. DePuy CH, Gronert S, Mullin A, Bierbaum VM (1990) J Am Chem Soc 112:8650–8655
14. Gronert S, Pratt LM, Mogali S (2001) J Am Chem Soc 123:3081–3091
15. Gronert S, Fagin AE, Okamoto K, Mogali S, Pratt LM (2004) J Am Chem Soc 126:12977–12983
16. Gronert S (2003) Acc Chem Res 36:848–857
17. Lum RC, Grabowski JJ (1992) J Am Chem Soc 114:9663–9664
18. Noest AJ, Nibbering NMM (1980) Adv Mass Spectrom 8:227–233
19. Bartmess JE, Hays RL, Khatri HN, Misra RN, Wilson SR (1981) J Am Chem Soc 103:4746–4751
20. Van Doren JM, Barlow SE, Depuy CH, Bierbaum VM (1987) Int J Mass Spectrom 81:85–100
21. Wille U, Dreessen T (2006) J Phys Chem A 110:2195–2203
22. Wille U, Tan JC-S, Mucke EK (2008) J Org Chem 73:5821–5830
23. Kyne SH, Schiesser CH, Matsubara H (2008) J Org Chem 73:427–434
24. Espinosa-Garcia J (1999) Chem Phys Lett 315:239–247
25. Linstrom PJ, Mallard WG (2005) NIST Chemistry WebBook, NIST Standard Reference Database Number 69. National Institute of Standards and Technology, Gaithersburg
26. Chase WM, Davies CA, Downey JJR, Frurip DJ, McDonald RA, Syverud AN (1985) JANAF Thermochemical Tables, 3rd ed., Parts I and II. J Phys Chem Ref Data Suppl 1
27. Becke AD (1993) J Chem Phys 98:5648–5652
28. Lee C, Yang W, Parr RG (1988) Phys Rev B 37:785–789
29. Parthiban S, de Oliveira G, Martin JML (2001) J Phys Chem A 105:895–904
30. Takahashi M, Tsutsui S, Sakamoto K, Kira M, Muller T, Apeloig Y (2001) J Am Chem Soc 123:347–348
31. Fukui K (1981) Acc Chem Res 14:363–368
32. Reed AE, Curtiss LA, Weinhold F (1988) Chem Rev 88:899–926
33. Frisch MJ, Trucks GW, Schlegel HB, Scuseria GE, Robb MA, Cheeseman JR, Montgomery JA, Vreven T, Kudin KN, Burant JC, Millam JM, Iyengar SS, Tomasi J, Barone V, Mennucci B, Cossi M, Scalmani G, Rega N, Petersson GA, Nakatsuji H, Hada M, Ehara M, Toyota K, Fukuda R, Hasegawa J, Ishida M, Nakajima T, Honda Y, Kitao O, Nakai H, Klene M, Li X, Knox JE, Hratchian HP, Cross JB, Bakken V, Adamo C, Jaramillo J, Gomperts R, Stratmann RE, Yazyev O, Austin AJ, Cammi R, Pomelli C, Ochterski JW, Ayala PY, Morokuma K, Voth GA, Salvador P, Dannenberg JJ, Zakrzewski VG, Dapprich S, Daniels AD, Strain MC, Farkas O, Malick DK, Rabuck AD, Raghavachari K, Foresman JB, Ortiz JV, Cui Q, Baboul AG, Clifford S, Cioslowski J, Stefanov BB, Liu G, Liashenko A, Piskorz P, Komaromi I, Martin RL, Fox DJ, Keith T, Al-Laham MA, Peng CY, Nanayakkara A, Challacombe M, Gill PMW, Johnson B, Chen W, Wong MW, Gonzalez C, Pople JA (2004) Gaussian 03, revision E.01. Gaussian Inc, Wallingford
34. DePuy CH, Bierbaum VM (1981) J Am Chem Soc 103:5034–5038
35. Applequist DE, Peterson AH (1961) J Am Chem Soc 83:862–865
36. Kapeller D, Barth R, Mereiter K, Hammerschmidt F (2007) J Am Chem Soc 129:914–923
37. Nobe Y, Arayama K, Urabe H (2005) J Am Chem Soc 127:18006–18007
38. Bierbaum VM, Depuy CH, Shapiro RH (1977) J Am Chem Soc 99:5800–5802
39. Kass SR, Filley JJ, Doren MV, Depuy CH (1986) J Am Chem Soc 108:2849–2852
40. Wiberg KB, Murcko MA(1987) J Phys Chem 91:3616-3620
41. Hammond GS (1955) J Am Chem Soc 77:334–338
42. Bento AP, Bickelhaupt FM (2008) J Org Chem 73:7290–7299
43. King GK, Maricq MM, Bierbaum VM, DePuy CH (1981) J Am Chem Soc 103:7133–7140
44. Allred AL (1961) J Inorg Nucl Chem 17:215–221
45. Jones WM, LaBar RA, Brinker UH, Gebert PH (1977) J Am Chem Soc 99:6379–6391
46. Moss RA, Fedorynski M, Shieh WC (1979) J Am Chem Soc 101:4736–4738
47. Moss RA, Munjal RC (1979) Tetrahedron Lett 19:4721–4724
48. Smith NP, Stevens IDR (1979) J Chem Soc Perkin Trans 2:1298–1308